

Photophysical and Photocatalytic Properties of AgInW_2O_8

Junwang Tang,^{*,†} Zhigang Zou,[‡] and Jinhua Ye^{*,†,§}

Ecomaterials Center, National Institute for Materials Science (NIMS), 1-2-1 Sengen, Tsukuba, Ibaraki 305-0047, Japan, Photoreaction Control Research Center (PCRC), National Institute of Advanced Industrial Science and Technology (AIST), Higashi, Tsukuba, Ibaraki 305-8565, Japan, and PRESTO, Japan Science and Technology Agency, 4-1-8 Honcho Kawaguchi, Saitama, Japan

Received: July 10, 2003; In Final Form: October 20, 2003

A photocatalyst, AgInW_2O_8 , with a layered structure was synthesized. The physical and photophysical properties of the photocatalyst were characterized by XRD, BET measurement, UV–visible diffuse reflectance, and photoluminescence, respectively. The photocatalytic properties of the photocatalyst for H_2 evolution with Pt cocatalyst from $\text{CH}_3\text{OH}/\text{H}_2\text{O}$ solution and O_2 evolution from AgNO_3 solution were observed under UV and visible light irradiation. The AgInW_2O_8 photocatalyst presented not only the activity of O_2 evolution but also the activity of H_2 evolution. Also the photocatalyst showed the ability to evolve H_2 from pure water under full arc irradiation. On the basis of all the results, the band structure of the photocatalyst was discussed.

Introduction

The discovery of an active photocatalyst for water splitting often attracts much attention since photoelectrochemical water splitting was reported over a TiO_2 electrode.¹ The fundamental steps for photocatalytic water splitting include (1) the generation of photogenerated electron–hole pairs in the semiconductor and (2) the separation of the charge carriers and the utilization of the charge carriers. The former is due to the excitation of a photoelectron from the valence band to the conduction band in the semiconductor. This process is strongly associated with the electronic structures of the semiconductor.² Some active photocatalysts were recently reported for water splitting under visible light or UV light irradiation based on the special electronic structure of the photocatalysts.^{2–6} So, the electronic structure of a photocatalyst plays a crucial role in determining the photocatalytic activity. On the other hand, a series of layered structure compounds showed high activity for water splitting under light irradiation,⁷ and this kind of structure was found to promote the generation and the separation of the charge carriers. This indicated that the crystal structure of a photocatalyst also heavily affects its photocatalytic activity.

WO_3 is a well-known photocatalyst for photocatalytic O_2 evolution.⁸ It does not show any activity for H_2 evolution under visible light or UV light irradiation, because its conduction band is below the H^+/H_2 potential level.⁹ Many efforts have been made to change the electronic structure of metal tungstates to realize photocatalytic H_2 evolution and simultaneously keep the ability of photocatalytic O_2 evolution. However, the results are very few except for the reports about $\text{Na}_2\text{W}_3\text{O}_{10}$ and $\text{Bi}_2\text{W}_2\text{O}_9$ with a low photocatalytic activity for H_2 and O_2 evolution under UV light irradiation.^{10,11} Meanwhile, some groups found that the photocatalysts containing the InO_6 octahedron showed a high activity for photocatalytic H_2 evolution under UV light and

visible light irradiation, which suggested that the In 5s level was above the H_2 reduction level in many semiconductors.^{2,12–14} On the basis of the consideration of the crystal structure and the electronic structure, here a AgInW_2O_8 photocatalyst was synthesized, which is characterized by a layered structure and includes the InO_6 octahedral network. The compound was also reported by Sato et al. in a Japanese domestic conference,^{2b} which we knew of by chance only very recently. In their work, Sato et al. reported the photocatalytic performance of the $\text{RuO}_2/\text{AgInW}_2\text{O}_8$ catalyst. Anyhow, it is important to know the effects of their crystal and electronic structures on the photophysical and photocatalytic properties. In the present work, we have carried out detailed studies on the crystal and electronic structures of the photocatalyst and clarified its photophysical properties via various experimental techniques. Photocatalytic water decomposition over the photocatalyst under different kinds of light irradiation was also investigated to test the validity of the material's design.

Experimental Section

AgInW_2O_8 was prepared by a solid-state reaction. High-purity Ag_2O , In_2O_3 , and WO_3 were mixed stoichiometrically and calcined at 823 K for 4 h, then at 1073 K for 24 h. The crystal structure of the samples was determined by the X-ray diffraction method with Cu K α radiation (JEOL JDX-3500 Tokyo, Japan). The diffuse reflectance spectra of the photocatalyst were measured by UV–visible spectrometer (UV-2500, Shimadzu, Japan). The surface area of the oxide was determined by BET measurement (Micromeritics-2360, Shimadzu, Japan) of nitrogen adsorption at 77 K. The photoluminescence (PL) spectra of the photocatalyst were detected with a spectrofluorometer (FR-6500, JASCO, Japan).

Photocatalytic H_2 and O_2 evolution were conducted with 0.5 g of photocatalyst suspended in a 270-mL solution. The reaction cell was an external irradiation Pyrex reactor, which was connected to a closed gas-circulating system. A 300-W Xe arc lamp was focused through a shutter window, and a cutoff filter (providing the visible light of different wavelength) and water filter (removing IR light irradiation) were placed between the

* Address correspondence to these authors. E-mail: jinhua.ye@nims.go.jp; tang.junwang@nims.go.jp.

[†] National Institute for Materials Science (NIMS).

[‡] National Institute of Advanced Industrial Science and Technology (AIST).

[§] Japan Science and Technology Agency.

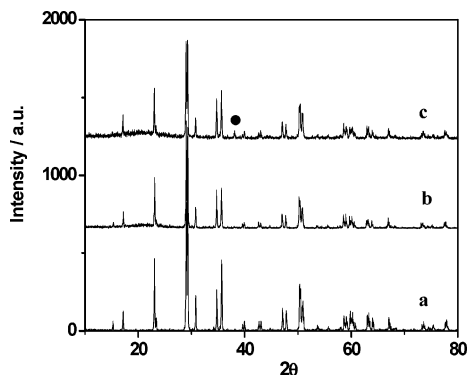


Figure 1. XRD spectra of AgInW_2O_8 before and after the photocatalytic water splitting: (a) before the photocatalytic reaction, (b) after the photocatalytic H_2 evolution, and (c) after the photocatalytic O_2 evolution. Metallic Ag (●) is indicated in spectra c.

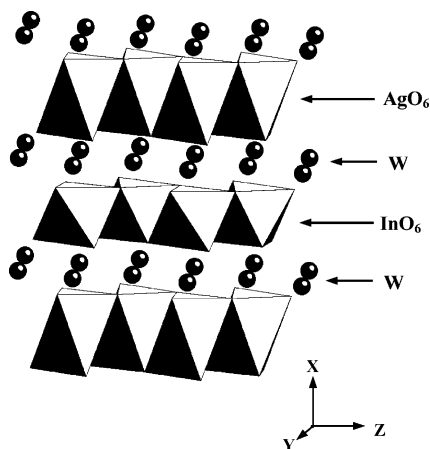


Figure 2. Schematic crystal structure of the AgInW_2O_8 photocatalyst.

Xe lamp and the reaction cell. Gas evolution was determined by a gas chromatograph with a TCD detector (GC-8A, Shimadzu, Japan), which was connected to the reaction system with a circulating line. $\text{NiO}(1.0 \text{ wt } \%)/\text{AgInW}_2\text{O}_8$ was prepared by impregnating the oxide with $\text{Ni}(\text{NO}_3)_2$ solution, and calcining at 823 K for 4 h. H_2 evolution reactions were performed in aqueous $\text{CH}_3\text{OH}/\text{H}_2\text{O}$ solution (50 mL of CH_3OH , 220 mL of H_2O) with cocatalyst Pt, where Pt was photodeposited on the photocatalyst with the precursor of H_2PtCl_6 . O_2 evolution reactions were performed in aqueous AgNO_3 solution without any cocatalyst (5 mmol of AgNO_3 , 270 mL of H_2O). Pure water splitting was performed over $\text{NiO}(1.0 \text{ wt } \%)/\text{AgInW}_2\text{O}_8$.

Results and Discussion

Structure. Figure 1 shows the X-ray powder diffraction pattern of the AgInW_2O_8 photocatalyst. It was found that the photocatalyst was well crystallized in a single phase.¹⁵ The schematic structure of AgInW_2O_8 is presented in Figure 2. The photocatalyst, belonging to the monoclinic system, space group $P2_1/c$, crystallizes in a layered crystal structure including the InO_6 octahedron and the AgO_6 octahedron. Among them, the AgO_6 octahedron is distorted and the InO_6 octahedron is somewhat prolate. The InO_6 octahedra connect by sharing edges to form a layer, and the AgO_6 octahedra form another layer. Tungsten atoms are located between the InO_6 layers and AgO_6 layers, like a sandwich. The lattice parameters of AgInW_2O_8 were refined by the least-squares method. The results of the refinement were as follows: $a = 10.32(2) \text{ \AA}$, $b = 5.80(1) \text{ \AA}$, $c = 5.03(1) \text{ \AA}$, and $\beta = 90.27(3)^\circ$, which were consistent with the report of Pakhomov et al.¹⁵

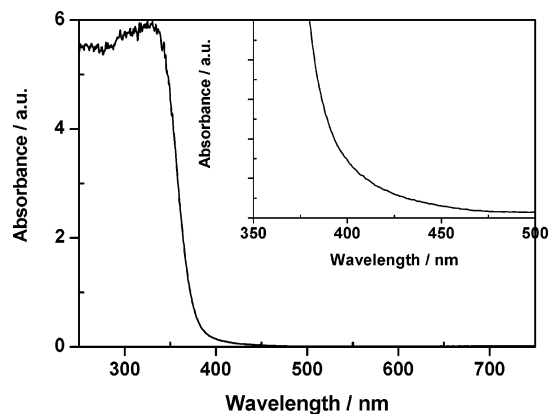


Figure 3. UV-visible diffuse reflectance spectra of AgInW_2O_8 with the inset providing an expanded view of the spectra from 350 to 500 nm.

Photophysical Properties. The UV-visible diffuse reflectance spectrum of the AgInW_2O_8 semiconductor is shown in Figure 3. It could be seen that the absorbance of the oxide extended to the visible light region from the inset in Figure 3. For a crystalline semiconductor, it is known that the optical absorption near the band edge follows the equation¹⁶

$$\alpha h\nu = A(h\nu - E_g)^n \quad (1)$$

in which α , ν , A , and E_g are absorption coefficient, light frequency, proportionality constant, and band gap, respectively. In the equation, n decides the characteristics of the transition in a semiconductor. The values of n and E_g were determined by the following steps: first, plot $\ln(\alpha h\nu)$ vs $\ln(h\nu - E_g)$, using an approximate value of E_g , and then determine the value of n with the slope of the straightest line near the band edge; second, plot $(\alpha h\nu)^{1/n}$ vs $h\nu$ and then evaluate the band gap E_g by extrapolating the straightest line to the $h\nu$ axis intercept. By using this method, the value of n for the oxide was determined as 2 from Figure 3. This means that the optical transitions for the oxide are indirectly allowed. The value of the band gap for the photocatalyst was determined as 3.12 eV.

The PL spectra of the semiconductor are useful to disclose the migration, transfer, and recombination processes of the photogenerated electron-hole pairs. The PL spectra of the AgInW_2O_8 photocatalyst at liquid N_2 conditions are presented in Figure 4 (see curves a' and b'). It was clear that there were two peaks, 375 and 555 nm in the PL spectra, which meant two recombination processes. The excitation spectra corresponding to the two emission spectra were also determined at 77 K (curves a and b in Figure 4). The total excitation spectra were in good agreement with the diffuse reflectance spectra (curve c in Figure 4). These spectra also indicated that there were two optical excitation processes, namely, two band gaps in the material. Among them, one was in the UV region, the other in the near-visible light region. The band structure of a transition metal oxide is generally defined by the d level of the transition metal and the O 2p level.¹⁷ Theoretical calculation also showed that the band features of a semiconductor containing InO_6 were dominated by the In 5s and O 2p levels.¹⁸ In the present photocatalyst, the Ag^+ ion has a similar electronic configuration and geometric position with the In^{3+} ion, indicating that the Ag 5s level is very close to the In 5s level. Recently, Kudo et al. reported the hybridized band of Ag 4d and O 2p as a preferable valence band for water splitting.^{19,20} Therefore, it is suggested that the band structure of the present photocatalyst consists of the Ag 4d, O 2p, as well as W 5d, In 5s, and Ag 5s

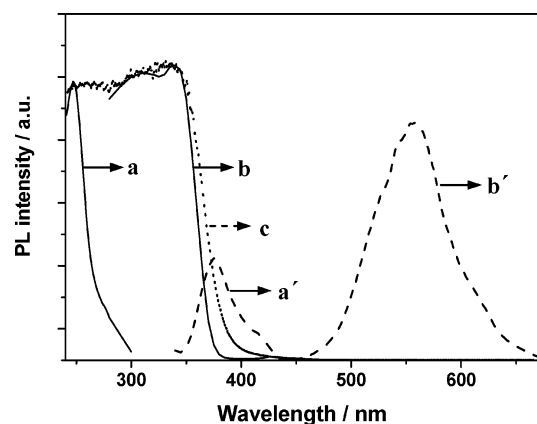


Figure 4. Photoluminescence spectra of AgInW_2O_8 at 77 K: (a) an excitation spectra monitored at 375 nm; (b) an excitation spectra monitored at 555 nm; and (c) a diffuse reflectance spectra (same as that in Figure 3); as well as the emission spectra excited at 250 nm (a') and at 370 nm (b').

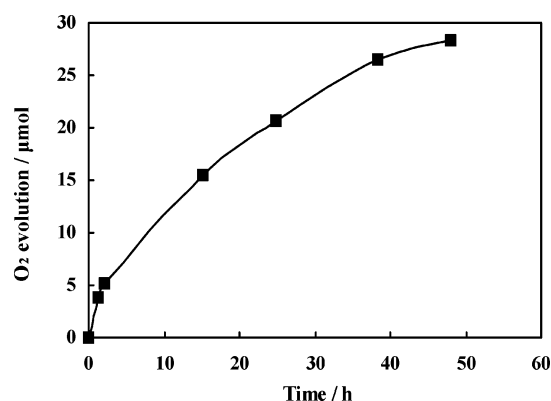


Figure 5. Photocatalytic O_2 evolution over AgInW_2O_8 under visible light ($\lambda > 420$ nm): catalyst, 0.5 g; AgNO_3 , 5 mmol; water, 270 mL.

levels. Among them, the hybridized band of Ag 4d and O 2p is the valence band, and the empty W 5d and the hybridized band of Ag 5s and In 5s are two possible conduction bands. The above-mentioned two optical excitation processes involved the electron excitation from the hybridized band of Ag 4d and O 2p to the W 5d level and to the hybridized band of Ag 5s and In 5s, respectively.

Photocatalytic Properties. The photocatalytic properties of the photocatalyst were investigated under Xe lamp irradiation with a 420-nm filter (visible light) and without any filter (full arc irradiation), respectively. Figure 5 represents photocatalytic O_2 evolution from AgNO_3 solution with the irradiation of visible light. The initial rate of the O_2 evolution was $3.6 \mu\text{mol/h}$ under visible light irradiation. With an increase in the reaction time, evolved O_2 increased. After 40 h, the O_2 evolution rate decreased remarkably, which was possibly because the metallic Ag from the AgNO_3 sacrificial reagent shielded the incident light and reduced the surface active sites of the photocatalyst. The crystal structure of the photocatalyst after photocatalytic O_2 evolution was detected by XRD as shown in Figure 1. It could be seen that the metallic Ag peak had appeared; similar results have been reported by Kudo et al.⁵ Photocatalytic H_2 evolution with Pt cocatalyst and $\text{CH}_3\text{OH}/\text{H}_2\text{O}$ was also carried out under visible light irradiation. However, no H_2 was detected.

The photocatalytic process is considered as the direct absorption of a photon, causing photogenerated electron transfer as well as forming the oxidized valence band and reduced conduction band. If the oxidized valence band is below the $\text{O}_2/\text{H}_2\text{O}$ potential level (1.23 V vs SHE, pH 0), O_2 evolution will

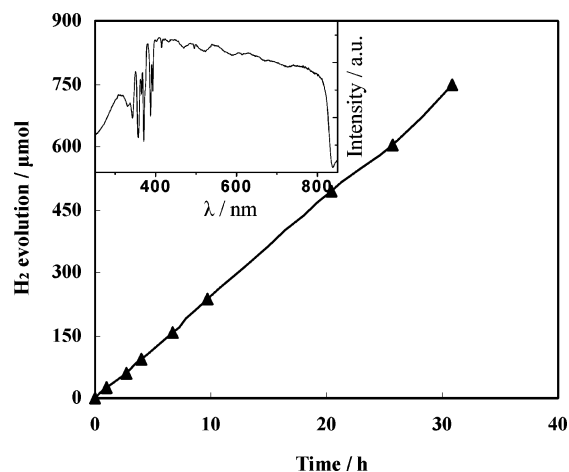


Figure 6. Photocatalytic H_2 evolution over AgInW_2O_8 under full arc irradiation: catalyst, 0.5 g; Pt cocatalyst, 0.2 wt %; CH_3OH , 50 mL; water, 220 mL. The inset is the reflectance spectrum of the visible reflection mirror used in the full arc Xe irradiation.

be possible. Similarly, if the reduced conduction band is above the H^+/H_2 potential level (0 V vs SHE, pH 0), H_2 evolution is also possible. The results of the photocatalytic water splitting indicated that the valence band of the AgInW_2O_8 photocatalyst meets the requirement of O_2 evolution under visible light irradiation. Namely, the hybridized band of the Ag 4d and O 2p level is more positive than the $\text{O}_2/\text{H}_2\text{O}$ potential level in the photocatalyst. However, the conduction band of the photocatalyst does not meet the requirement of H_2 evolution under visible light irradiation. The present conduction band might be one of the W 5d and the hybridized band that of Ag 5s and In 5s.

With use of full arc irradiation of the Xe lamp to photocatalytically decompose water, H_2 evolution with the aid of the relevant sacrificial reagents is shown in Figure 6. The inset in Figure 6 is the reflectance spectrum of the visible reflection mirror used in the full arc Xe irradiation. It is obvious that the full arc irradiation contains both UV light and visible light irradiation, suggesting the light intensity under full arc was somewhat stronger than that under visible light. During the experimental period, H_2 evolution increased linearly. The average rate of H_2 evolution was $25 \mu\text{mol/h}$. The turnover number (TN), calculated by eq 2, exceeded 2 after 30 h of reaction time under full arc irradiation. The turnover number is usually defined as the number of a product divided by the number of active sites on the surface of a catalyst. It is difficult to determine the number of active sites for heterogeneous photocatalysts. Here we adopted the total amount of the catalyst as the number of active sites to ensure the reliability of the evaluation. The turnover number is enough to prove that the reaction is photocatalysis, not a photocorrosion.

$$\text{TN} = \frac{\text{number of reacted photoelectrons}}{\text{amount of } \text{AgInW}_2\text{O}_8} = \frac{\text{molar quantity of evolved } \text{H}_2 \times 2}{\text{molar quantity of } \text{AgInW}_2\text{O}_8} \quad (2)$$

As shown in Figure 6, although the full arc only contains a small quantity of UV light, the photocatalyst presented a high activity for H_2 evolution when irradiating with the full arc instead of visible light. This meant that the photocatalyst for H_2 evolution is responsive to UV light. So, we observed H_2 evolution under a high-pressure Hg lamp that strongly emits UV light. The rate of H_2 evolution was nearly $100 \mu\text{mol/h}$, and the turnover number exceeded 11 after 40 h of reaction time.

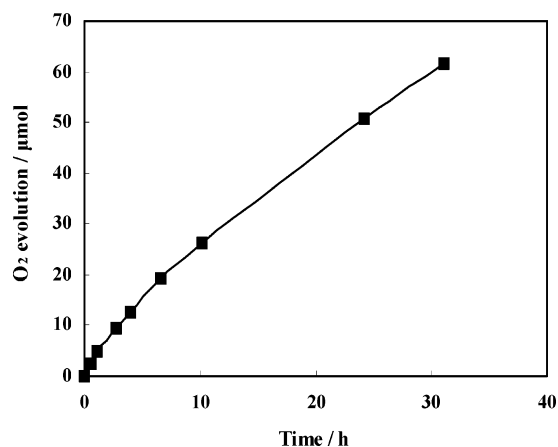


Figure 7. Photocatalytic O₂ evolution over AgInW₂O₈ under full arc irradiation: catalyst, 0.5 g; AgNO₃, 5 mmol; water, 270 mL.

TABLE 1: H₂ and O₂ Evolution under Different Light Irradiation

light source	light irradiation	H ₂ evolution (μmol/h)	O ₂ initial evolution (μmol/h)
Xe lamp with 420-nm filter	visible light		3.6
Xe lamp without filter	full arc	25	5
high-pressure Hg lamp	UV light	100	266

All these results indicated that H₂ was evolved photocatalytically in this work. Figure 7 represents photocatalytic O₂ evolution under full arc irradiation. O₂ evolution also increased with time. Its tendency was similar to the results obtained under visible light irradiation. The initial rate of O₂ evolution was 5 μmol/h, which was higher than that under visible light. In view of the increasing light intensity, it is reasonable that the activity of the photocatalyst for O₂ evolution under full arc would be higher than that under visible light. On the other hand, the above results indicated that the conduction band and the valence band of the AgInW₂O₈ photocatalyst meet the requirements of H₂ evolution and O₂ evolution potential levels under full arc irradiation, respectively. The crystal structure of the photocatalyst after photocatalytic H₂ evolution under full arc was detected by XRD, which is shown in Figure 1. It could be seen that the crystal structure of the photocatalyst was not changed after the photocatalytic reaction.

Band Structure. Table 1 summarizes photocatalytic H₂ and O₂ evolution under different light irradiation. From these results, it is obvious that the hybridized band of Ag 4d and O 2p in the photocatalyst is more positive than the O₂/H₂O potential level. However, between the W 5d and the hybridized band of Ag 5s and In 5s, only one is more negative than the H⁺/H₂ potential level. It is known that tungsten oxide is unable to meet the H⁺ reduction potential, whereas the potential of the In 5s level in InO₆ octahedra was suitable to H⁺ reduction, which has been proven by the photoactivities of many semiconductors, such as MIn₂O₄ (M = Ca, Sr, Ba), InMO₄ (M = V, Nb, Ta), and so on.^{2,12–14} Also, the Ag 5s level was determined to be more negative than the H⁺/H₂ potential level.¹⁹ So it is reasonable to deem that the hybridized band of Ag 5s and In 5s is more negative than the H⁺/H₂ potential level. The band structure of AgInW₂O₈ is suggested as shown in Figure 8. Under visible light irradiation, the photogenerated electron transfers from the hybridized band of Ag 4d and O 2p to the W 5d level, so that H₂ evolution is impossible while O₂ evolution is possible. Under full arc irradiation, with increasing light energy, the photogenerated electron can transfer from the hybridized band of Ag

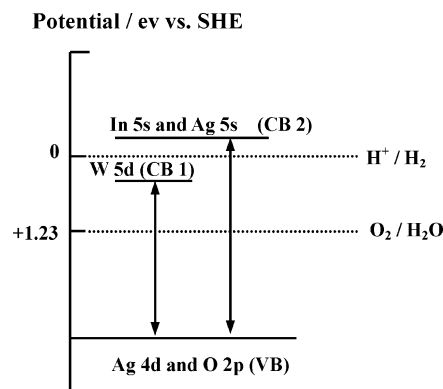


Figure 8. Suggested diagram of the band structure of AgInW₂O₈. VB is the valence band; CB is the conduction band.

4d and O 2p to the hybridized band of Ag 5s and In 5s in addition to the W 5d level. The CB and VB potential levels meet the requirements of H₂ and O₂ evolution this time, and so H₂ and O₂ evolution are reasonable.

Considering the PL of the photocatalyst, the peak a' was attributed to the recombination of the photoelectron in the hybridized band of Ag 5s and In 5s with the photohole in the hybridized band of Ag 4d and O 2p, while the peak b' was the recombination of the photoelectron in the W 5d level with the photohole in the hybridized band of Ag 4d and O 2p. The PL spectral intensity often indicates the recombination rate of the electron–hole.²¹ The PL intensity of the photocatalyst in the UV region (peak a') was much weaker than that in the visible light region (peak b'). It suggested that the photoelectrons excited under UV irradiation could be transferred more easily to other substances instead of recombining with the photoholes compared with that under visible irradiation. This was attributed to the InO₆ and the AgO₆ layered structure, which was beneficial to the transfer of electrons to the surface of the photocatalyst along the layered network. Many reports have also shown that the photocatalysts containing a similar network had a high activity for the photocatalytic water splitting.^{12–14} Alternatively, some photoelectrons excited to the hybridized band of Ag 5s and In 5s could transfer to the W 5d level and then recombine with the photoholes in the hybridized band of Ag 4d and O 2p. This process could also decrease the PL spectra intensity in the UV region and increase it in the visible light region.

Splitting Pure Water. From the above results on the band structure of AgInW₂O₈, there is a possibility for the photocatalytic decomposition of pure water over the oxide. This study was performed over NiO(1.0 wt %)/AgInW₂O₈ under full arc irradiation (shown in Figure 9). The H₂ evolution rate was about 12 μmol/g per h in the first run. After 22 h, the dark experiment was conducted, and the H₂ evolution rate was zero. Turning on the Xe lamp, H₂ was continuously evolved again, the reaction rate was close to that in the first run. Here, the turnover number, in terms of reacted electrons relative to the number of Ni atoms loaded on the surface of the sample, reached 8 during the 44 h reaction time, suggesting that the reaction occurred catalytically. The above results indicated that pure water was photocatalytically decomposed under full arc irradiation. O₂ evolution was not detected in this experiment. The same phenomenon was also observed over InMO₄ (M = V, Nb, Ta) and TiO₂.^{9,12,13} Some researchers have found that there are both physisorbed and chemisorbed O₂ molecules on the surface of TiO₂ by low-energy photon irradiation, where the physisorbed O₂ is produced through the neutralization of chemisorbed O₂[−] species by photoholes.^{9,22} Zou et al. measured the DC magnetic suscepti-

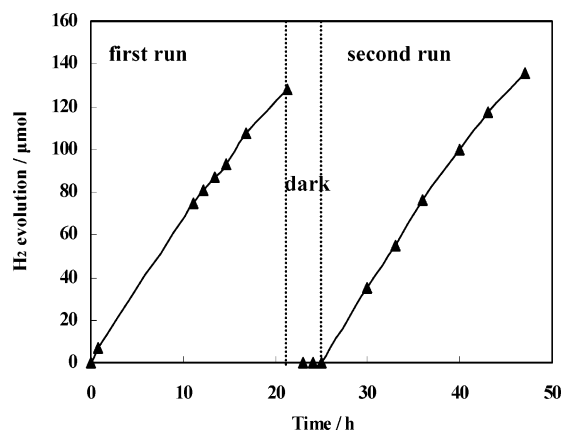


Figure 9. Photocatalytic decomposition of pure H_2O over $\text{NiO}/\text{AgInW}_2\text{O}_8$ under full arc irradiation: catalyst, 0.5 g; NiO , 1.0 wt %; water, 270 mL.

bilities of the $\text{Bi}_2\text{InNbO}_7$ photocatalyst with the InO_6 octahedron before and after the photocatalytic reaction.¹⁴ They found that the magnetic susceptibilities of the $\text{Bi}_2\text{InNbO}_7$ photocatalyst after the photocatalytic reaction developed an obvious broad peak around 50 K, which was attributed to the antiferromagnetic ordering of adsorbed oxygen on the surface of the sample. Although the relevant investigation was not conducted over the AgInW_2O_8 photocatalyst, we can speculate that the phenomenon of O_2 adsorption observed over the above photocatalysts took place on the surface of the AgInW_2O_8 photocatalyst. The BET measurement showed that the present photocatalyst had a very low surface area ($0.44 \text{ m}^2/\text{g}$), which indicated the possibility of greatly increasing photocatalytic activity by increasing the surface area of the photocatalyst.

Conclusions

In the present work a photocatalyst, AgInW_2O_8 , was synthesized based on the control of electronic and crystal structure. The photocatalyst is a semiconductor with a sandwich-like structure containing InO_6 and AgO_6 octahedral layers. Its photophysical and photocatalytic properties were observed. The photocatalyst showed not only photocatalytic O_2 evolution but also photocatalytic H_2 evolution. On the basis of these experimental results, a possible band structure was suggested, where the valence band of the photocatalyst was mainly composed of the hybridized band of Ag 4d and O 2p and two conduction bands, composed of the W 5d level and the hybridized band of Ag 5s and In 5s, respectively. O_2 and H_2 evolution over

AgInW_2O_8 was ascribed to photogenerated electron transfer from the hybridized band of Ag 4d and O 2p to the W 5d level under visible light and to the hybridized band of Ag 5s and In 5s under full arc irradiation, respectively. Furthermore, the photocatalyst showed good activity to decompose pure water under full arc irradiation. In addition, the synthesis of the present photocatalyst provides some useful insights for the design of new photocatalysts for the photocatalytic H_2 and O_2 evolution. The modification of the AgInW_2O_8 photocatalyst is being investigated further to realize pure water splitting under visible light irradiation.

Acknowledgment. This work was supported by the Grant-in-Aid for the Creation of Innovations thorough Business-Academic-Public Sector Cooperation, Japan.

References and Notes

- (1) Fujishima, A.; Honda, K. *Nature* **1972**, 238, 37.
- (2) (a) Sato, J.; Saito, N.; Nishiyama, H.; Inoue, Y. *J. Phys. Chem. B* **2001**, 105, 6061. (b) Sato, J.; Saito, N.; Nishiyama, H.; Inoue, Y. *Abstr. Catal. Soc. Jpn. Meet.* **2002**, 96 (in Japanese).
- (3) Zou, Z.; Ye, J.; Sayama, K.; Arakawa, H. *Nature* **2001**, 414, 625.
- (4) (a) Hitoki, G.; Takata, T.; Kondo, J. N.; Hara, M.; Kobayashi, H.; Domen, K. *Chem. Commun.* **2002**, 1698. (b) Kasahara, A.; Nukumizu, K.; Hitoki, G.; Takata, T.; Kondo, J. N.; Hara, M.; Kobayashi, H.; Domen, K. *J. Phys. Chem. A* **2002**, 106, 6750.
- (5) Kudo, A.; Omori, K.; Kato, H. *J. Am. Chem. Soc.* **1999**, 121, 11459.
- (6) Khan, S. U. M.; Al-Shahry, M.; Ingler, W. B., Jr. *Science* **2002**, 297, 2243.
- (7) (a) Kudo, A.; Tanaka, A.; Domen, K.; Maruya, K.; Aika, K.; Onishi, T. *J. Catal.* **1998**, 111, 67. (b) Takata, T.; Tanaka, A.; Hara, M.; Kondo, J. N.; Domen, K. *Catal. Today* **1998**, 44, 17.
- (8) Darwent, J. R.; Mills, A. *J. Chem. Soc., Faraday Trans.* **1982**, 78, 359.
- (9) Linsebigler, A. L.; Lu, G.; Yates, T. J., Jr. *Chem. Rev.* **1995**, 95, 735.
- (10) Kudo, A.; Kato, H. *Chem. Lett.* **1997**, 421.
- (11) Kudo, A.; Hiji, S. *Chem. Lett.* **1999**, 1103.
- (12) (a) Ye, J.; Zou, Z.; Oshikiri, M.; Matsushita, A.; Shimoda, M.; Imai, M.; Shishido, T. *Chem. Phys. Lett.* **2002**, 356, 221. (b) Yin, J.; Zou, Z.; Ye, J. *J. Phys. Chem. B* **2003**, 107, 61.
- (13) Zou, Z.; Ye, J.; Arakawa, H. *Chem. Phys. Lett.* **2000**, 332, 271.
- (14) Zou, Z.; Ye, J.; Arakawa, H. *J. Mol. Catal. A: Chem.* **2001**, 168, 289.
- (15) Pakhomov, V. I.; Fedorov, P. M.; Okunera, A. S.; Sorokina, O. V. *Koord. Khim.* **1977**, 3, 765.
- (16) Butler, M. A. *J. Appl. Phys.* **1977**, 48, 1914.
- (17) Scaife, D. E. *Sol. Energy* **1980**, 25, 41.
- (18) (a) Schinzer, C.; Heyd, F.; Mater, S. F. *J. Mater. Chem.* **1999**, 9, 1569. (b) Odaka, H.; Iwata, S.; Taga, N.; Ohnishi, S.; Kaneta, Y.; Shigesato, Y. *Jpn. J. Appl. Phys.* **1997**, 36, 5551.
- (19) Kato, H.; Kobayashi, H.; Kudo, A. *J. Phys. Chem. B* **2002**, 106, 12441.
- (20) Kudo, A.; Tsuji, I.; Kato, H. *Chem. Commun.* **2002**, 1958.
- (21) Li, F. B.; Li, X. Z. *Appl. Catal. A* **2002**, 228, 15.
- (22) Yanagisawa, Y.; Ota, Y. *Surf. Sci.* **1991**, 254, L433.